Jet Dynamics and Stability

Nektarios Vlahakis, University of Athens

JETSET FP6, “Jet Simulations, Experiments and Theory” 10 years later,
what would have been the continuation of the works related to jet dynamics?

- *Two-component jet simulations. I. Topological stability of analytical MHD outflow solutions*,
Matsakos Titos, Tsinganos, K., Vlahakis, N., Massaglia, S., Mignone, A., & Trussoni, E. 2008, A&A, 477, 521
- *Resistive jet simulations extending radially self-similar magnetohydrodynamic models*,
Čemeljić Miki, Gracia, J., Vlahakis, N., & Tsinganos, K. 2008, MNRAS, 389, 1022
- *Stability and structure of analytical MHD jet formation models with a finite outer disk radius*,
Stute Matthias, Tsinganos, K., Vlahakis, N., Matsakos Titos, & Gracia, J. 2008, A&A, 491, 339
- *Two-component jet simulations. II. Combining analytical disk and stellar MHD outflow solutions*,
Matsakos Titos, Massaglia, S., Trussoni, E., Tsinganos, K., Vlahakis, N., Sauty, C., & Mignone, A. 2009, A&A, 502, 217
- *Comparison of synthetic maps from truncated jet-formation models with YSO jet observations*,
Stute Matthias, Gracia, J., Tsinganos, K., & Vlahakis, N. 2010, A&A, 516, A6
- *Velocity asymmetries in YSO jets. Intrinsic and extrinsic mechanisms*,
Matsakos Titos, Vlahakis, N., Tsinganos, K., Karampelas, K., Sauty, C., Cayatte, V., Matt, S. P., Massaglia, S., Trussoni, E., & Mignone, A. 2012, A&A, 545, A53
- *Large resistivity in numerical simulations of radially self-similar outflows*,
Čemeljić Miki, Vlahakis, N., & Tsinganos, K. 2014, MNRAS, 442, 1133
- *3D simulations of disc winds extending radially self-similar MHD models*,
Stute Matthias, Gracia, J., Vlahakis, N., Tsinganos, K., Mignone, A., & Massaglia, S. 2014, MNRAS, 439, 3641

common ingredient:
a radially self-similar analytical solution for the disk-wind (Vlahakis et al 2000)

JETSET-postdoc works:
extend the solution by relaxing various assumptions/shortcomings:

geometrical shortcomings of radial self-similarity:

- singularity on jet axis (solved by Titos)
- the flow extends to radial infinity (solved by Matthias)

assumption of infinite conductivity (relaxed by Miki)
assumption of axisymmetry (relaxed by Matthias)

the solution is very robust!
only slight modifications even in 3D extensions

Can be used to test analytical ideas on how MHD works

Stute et al 2014

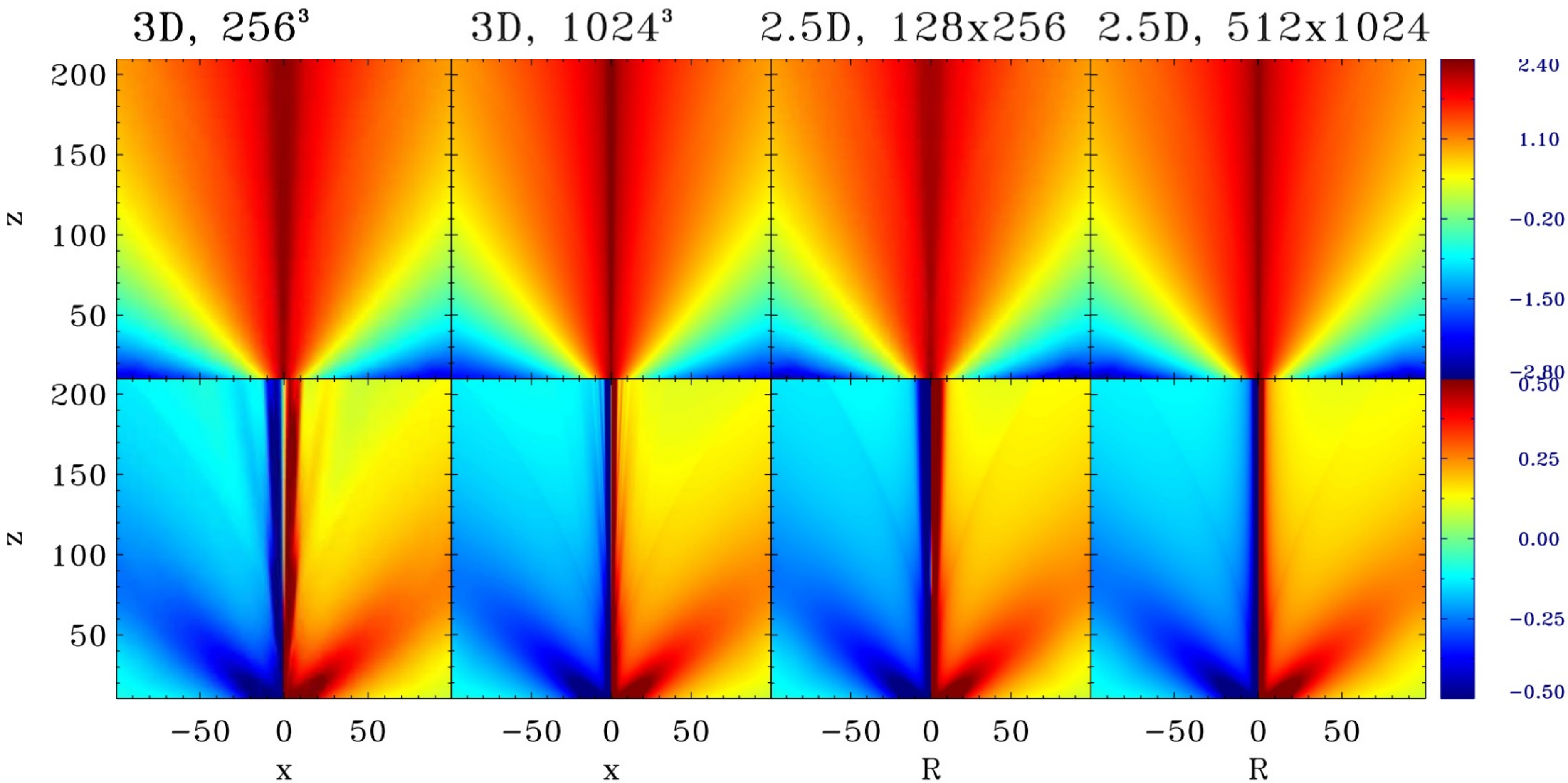

$\log(v_z)$ (top row) and v_ϕ (bottom) for 3D (two first columns) and axisymmetric simulations

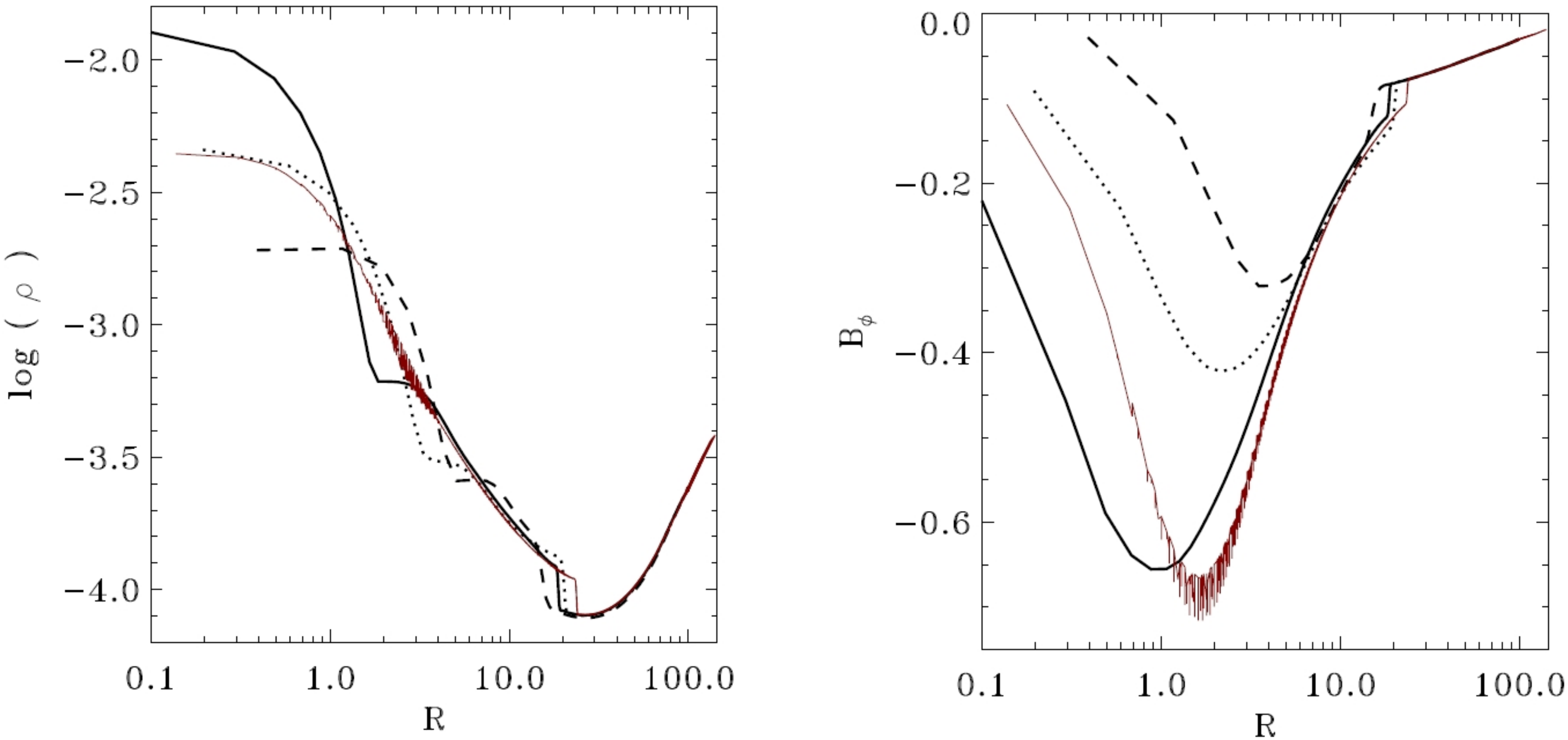

log (ρ)
−2.0
−2.5
−3.0
−3.5
−4.0
0.1
1.0
10.0
100.0
R
B$_\phi$
0.0
−0.2
−0.4
−0.6
0.1
1.0
10.0
100.0
R

Outline

analytical ideas on how MHD works

- magnetic acceleration
  the bunching function and a toy model
- why stable to current-driven instabilities?

magnetic acceleration

- simplified momentum equation along the flow

$$\rho \frac{dV}{dt} = -\frac{B_\phi}{4\pi\varpi} \frac{\partial}{\partial \ell} (\varpi B_\phi)$$

(RHS sum of magnetic pressure+tension – ignore gravity, pressure
ϖ= cylindrical distance)

- simplified Ferraro's law (ignore V_ϕ – small compared to $\varpi\Omega$)

$$V_\phi = \varpi\Omega + V B_\phi / B_p \quad \Leftrightarrow \quad B_\phi \approx -\frac{\varpi\Omega B_p}{V}$$

(Ω is an integral)

- combine the two and use the mass-to-magnetic flux integral $\Psi_A = \dfrac{4\pi\rho V}{B_p}$

$$m \frac{dV}{dt} = -\frac{\partial}{\partial \ell} \left(\frac{S}{V} \right) , \quad m = \frac{\Psi_A}{A\Omega^2} , \quad S = \frac{\varpi^2 B_p}{A}$$

(A is the magnetic flux – integral)

bunching function $S = \varpi^2 B_p / A$

using the definition of A, $$S = \frac{2\pi\varpi^2 B_p}{\int \boldsymbol{B}_p \cdot d\boldsymbol{a}}$$

thus S measures the ratio of the local over the mean poloidal magnetic field

it measures how bunched are the fieldlines at a given point

its variation along the flow measures the expansion of the flow,

$$S = \frac{2\pi\varpi\delta\ell_\perp B_p}{A}\frac{\varpi}{\delta\ell_\perp} \propto \frac{\varpi}{\delta\ell_\perp}$$

if $\delta\ell_\perp/\varpi$ increases, S decreases

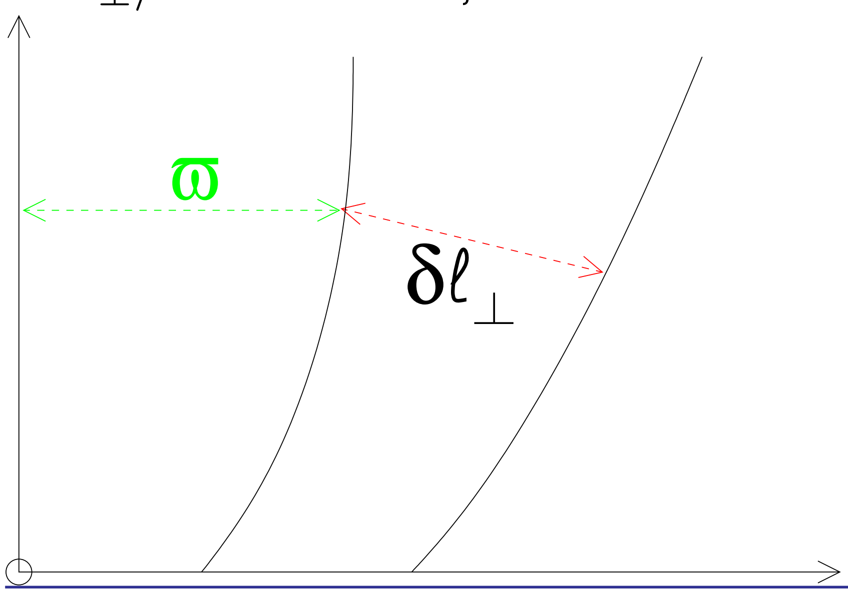

if $\delta\ell_\perp/\varpi$ decreases, S increases

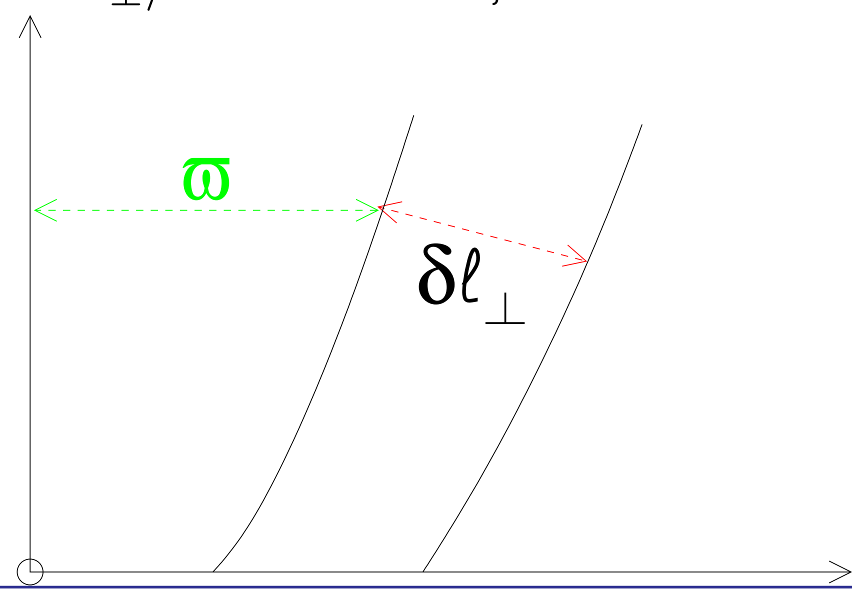

toy model

$$m\frac{dV}{dt} = -\frac{\partial}{\partial \ell}\left(\frac{S}{V}\right)$$

motion of a mass $m = \frac{\Psi_A}{A\Omega^2}$ in a velocity-dependent potential $\frac{S}{mV}$

corresponding energy integral = Bernoulli $\frac{V^2}{2} + \frac{S}{mV} = E$

potential $\frac{S}{mV}$ = square of the local fast-magnetosonic speed $V_f^2 = \frac{B^2}{4\pi\rho}$

The equation of particle motion can be written as a de-Laval nozzle equation

$$\frac{dV}{d\ell} = \frac{V\frac{dS}{d\ell}}{S - mV^3}, \qquad \frac{1}{S} \propto \frac{\delta\ell_\perp}{\varpi}$$

fast critical point $S|_{\rm fast} = S_{\rm max}, \quad V|_{\rm fast} = \left(\frac{S|_{\rm fast}}{m}\right)^{1/3}$

using the energy integral $E = \frac{3}{2}V|^2_{\rm fast}$

Vlahakis et al 2000

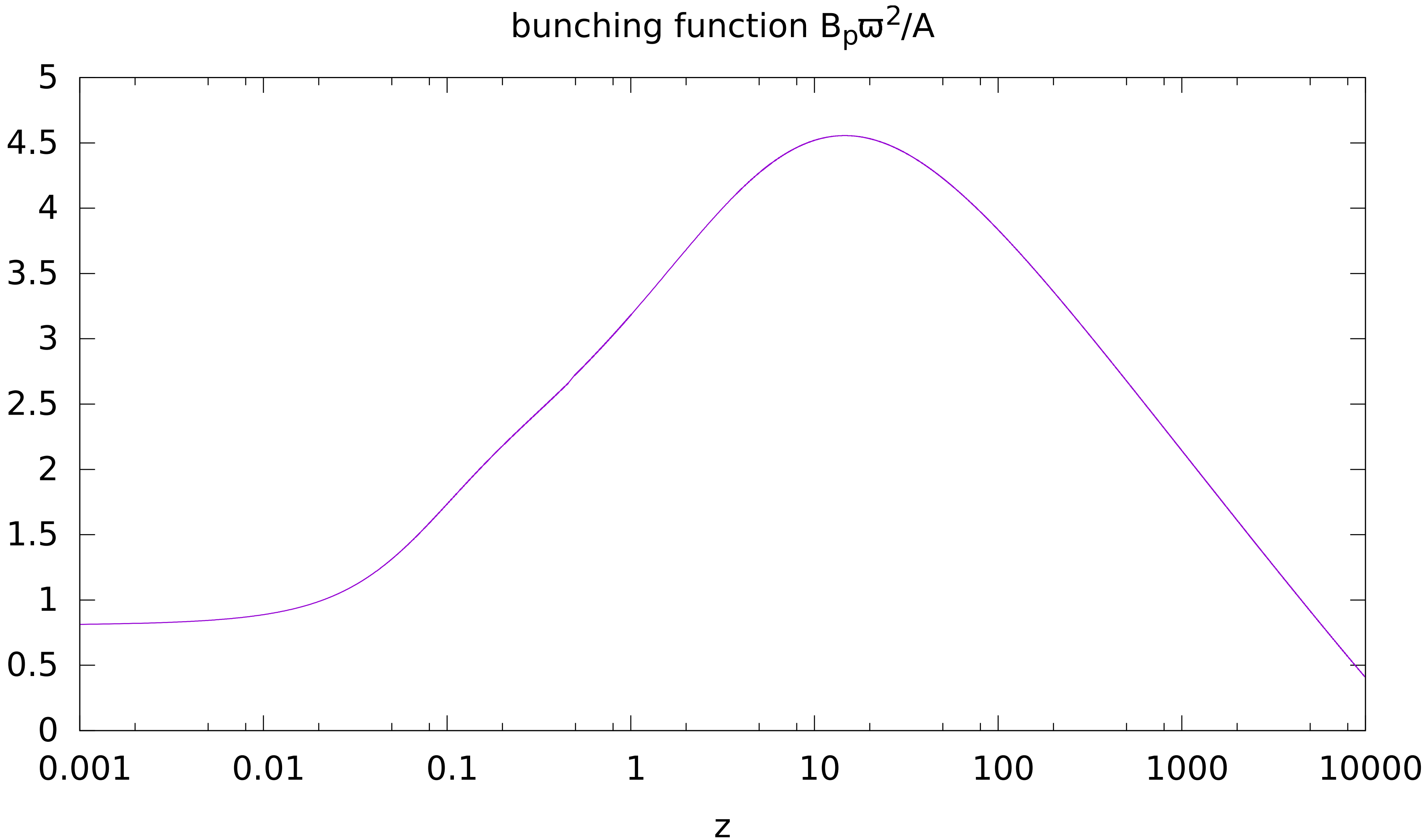

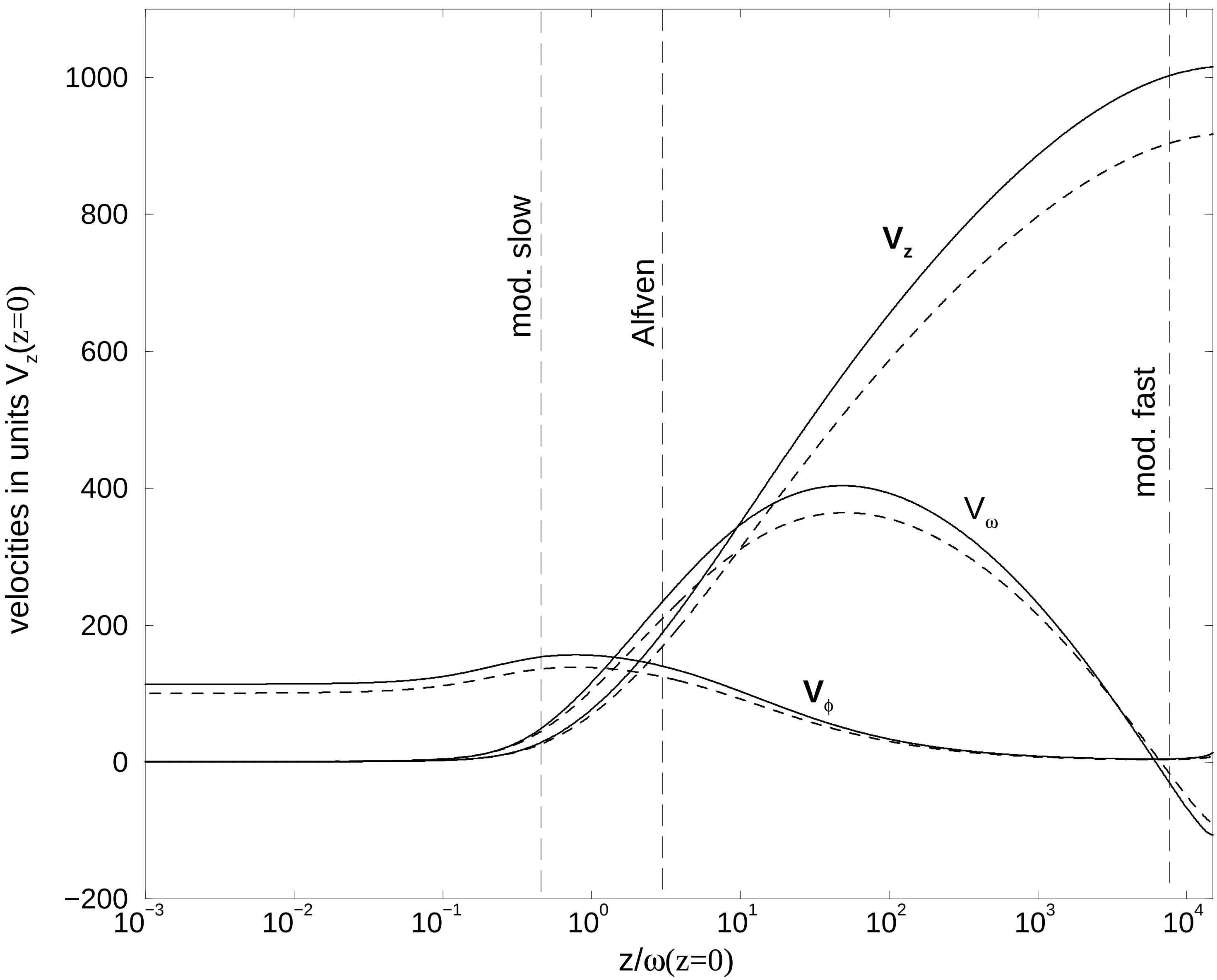

velocities in units $V_z(z=0)$
1000
800
600
400
200
0
−200
10^{-3}
10^{-2}
10^{-1}
10^{0}
10^{1}
10^{2}
10^{3}
10^{4}
$z/\omega(z=0)$
mod. slow
Alfven
mod. fast
V_z
V_ω
V_ϕ

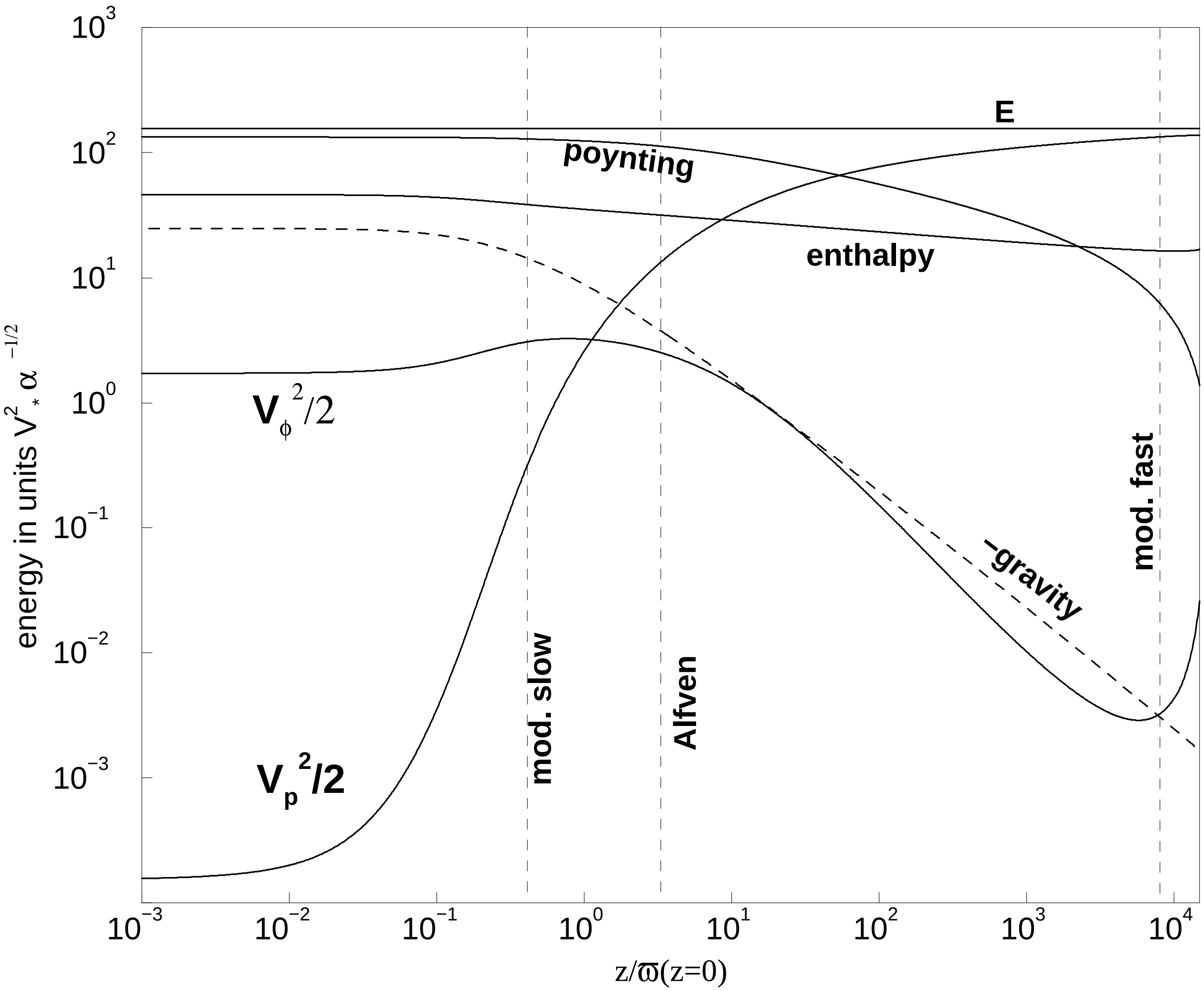

E
poynting
enthalpy
$V_\phi^2/2$
$V_p^2/2$
−gravity
mod. slow
Alfven
mod. fast
energy in units $V_*^2\,\alpha^{-1/2}$
$z/\varpi(z=0)$

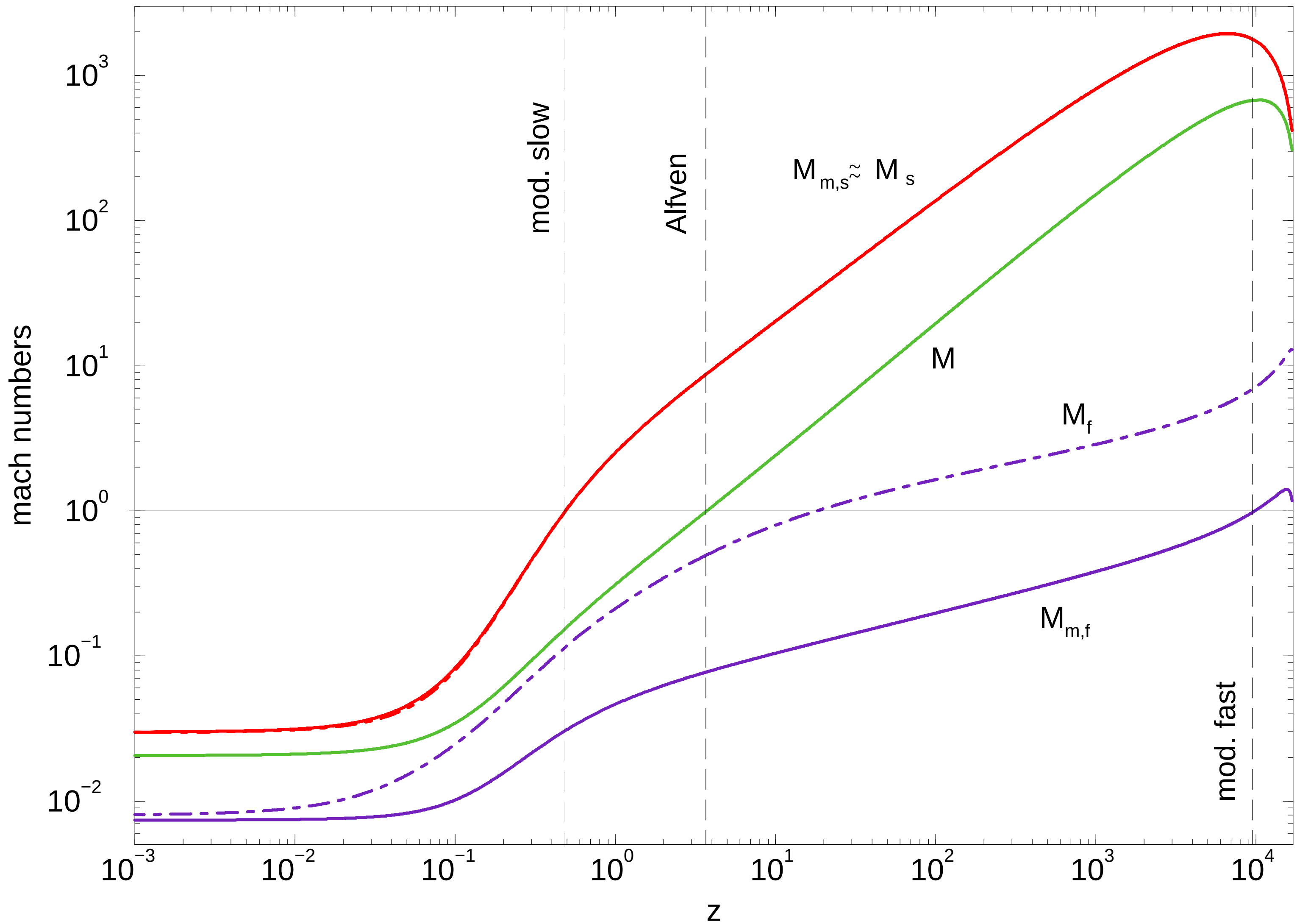

mach numbers
z
mod. slow
Alfven
mod. fast
$M_{m,s} \approx M_s$
M
M_f
$M_{m,f}$
10^{3}
10^{2}
10^{1}
10^{0}
10^{-1}
10^{-2}
10^{-3}
10^{-2}
10^{-1}
10^{0}
10^{1}
10^{2}
10^{3}
10^{4}

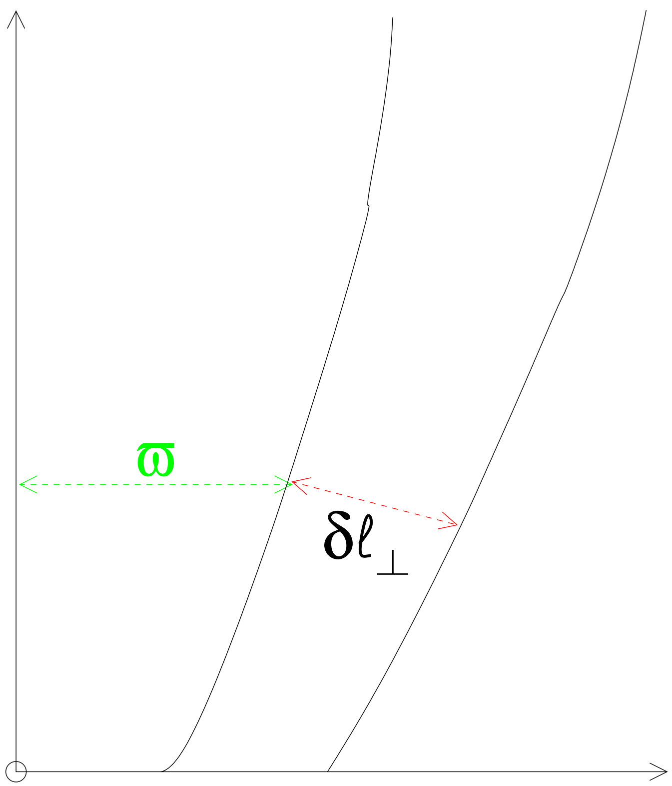

first S increases then decreases (differential collimation)

$S_\infty \sim 1$ so the Bernoulli integral

$$\frac{V_\infty^2}{2} + \frac{S_\infty}{mV_\infty} = E \quad \Leftrightarrow$$

$$\frac{(V_\infty / V|_{\rm fast})^2}{2} + \frac{S_\infty / S_{\rm max}}{V_\infty / V|_{\rm fast}} = \frac{3}{2}$$

gives the value of V_∞

higher $S_{\rm max}$ $\rightarrow$ higher acceleration efficiency

in V00 $S_{\rm max} \approx 4.5$ and acceleration efficiency $\gtrsim 90\%$

transfield force-balance

the transfield force-balance determines the flow shape and consequently the spatial dependence of acceleration

its approximate form in the superAlfvénic regime is

$$V^2\frac{\varpi}{\mathcal{R}} \approx -\varpi V_f^2 \hat{n}\cdot\nabla\ln(\varpi B) \sim V_f^2$$

$\mathcal{R} =$ curvature radius of poloidal lines, $\hat{n} =$ unit vector normal to lines

Since the potential of the Bernoulli integral is V_f^2, we connect the geometry with the speed (or the efficiency of the acceleration $\zeta = V^2/2E$)

$$V^2\frac{\varpi}{\mathcal{R}} \sim E - \frac{V^2}{2} \qquad \Leftrightarrow \qquad \zeta \equiv \frac{V^2}{2E} = \frac{1}{1+2\varpi/\mathcal{R}}$$

for power-law poloidal filedline shape $z \propto \varpi^b$

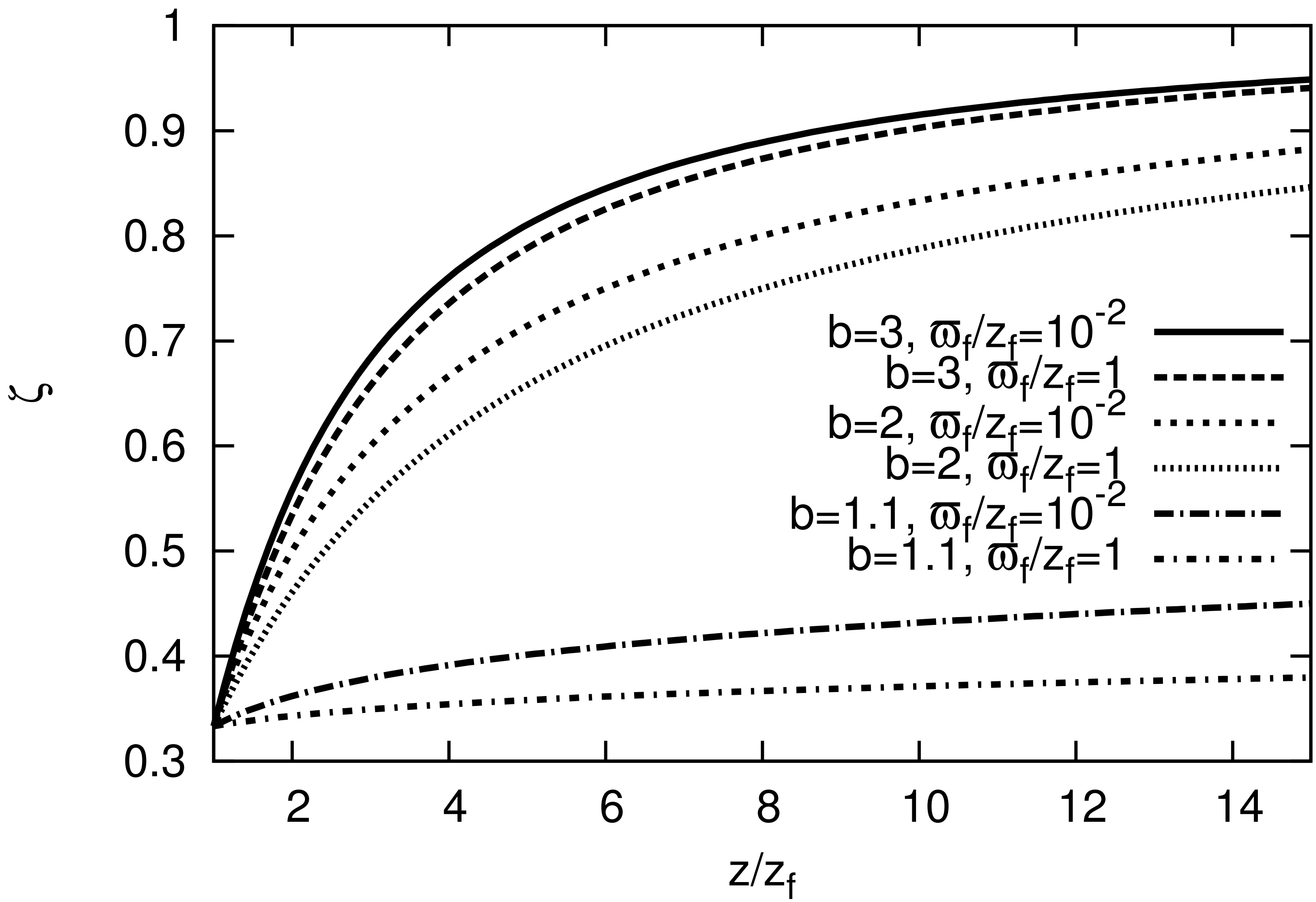

stronger collimation $\rightarrow$ faster acceleration

(V00 has $b \sim 1.3$)

Stability

linear analysis gives typical growth times of current-driven instabilities
a few Alfvénic crossing times $\tau \sim \frac{10\varpi}{V_f}$ (e.g. Appl, Lery & Baty 2000)

$V_f^2 =$ potential $= \frac{S}{mV}$ with $m = \frac{S_{\rm max}}{V|^3_{\rm fast}} = \frac{S_{\rm max}}{(2E/3)^{3/2}}$

$$V\tau \sim 10\varpi \left(\frac{3V^2}{2E}\right)^{3/4} \left(\frac{S_{\rm max}}{S}\right)^{1/2}$$

at infinity $V_\infty \sim \sqrt{2E}$, $S_\infty \sim 1$ so

$$V_\infty \tau \sim 10\varpi \times 3^{3/4} S_{\rm max}^{1/2} \sim 50\varpi$$

summary – next steps

- a single parameter ($S_{\rm max}$) defines the magnetic acceleration efficiency and the stability properties

- efficiently accelerated jets are much more stable to CDIs

- what controls the increase of S and its maximum value
  - magnetic field distribution in the disk surface?
  - simplified model for the combination transfield $(\varpi/\mathcal{R})$+ S

- 3-D simulations of interactions with environment – stability

- effects of finite resistivity in outflows (various models for resistivity)